

Biologically-inspired Coordination of Multiple UAVs using Sliding Mode Control

Young Hwan Chang, Claire Tomlin and Karl Hedrick

Abstract— We consider the problem of prey (evader) hunting for single or multiple Unmanned Aircraft Vehicles (UAVs) based on biologically-inspired predator-prey behavior. First, we apply sliding mode control (SMC) to a single predator/single prey model. Next, we propose motion synchronization of multiple UAVs to hunt prey effectively. The proposed motion control scheme is formulated and synchronization is proved. Also, numerical examples demonstrate the performance of the proposed SMC controller and synchronization of multiple UAVs. Therefore, a biologically-inspired strategy of multiple UAVs with synchronization might be a possible approach to effectively hunt other UAVs.

I. INTRODUCTION

Formation flight control of multiple Unmanned Aircraft Vehicles (UAVs) has been an active research topic for many years, since it supports many practical applications, such as surveillance, forecasting weather, damage assessment, and search and rescue [1][2][3]. Also, the research on multi-agent control has drawn significant inspiration from interaction rules in social animals and insects: aggregation, foraging, flocking, formation flight and cooperation [4][5][6][7]. In this paper, we follow the line of inquiry by asking how predators can pursue prey effectively and what kind of strategies can be applied to hunt prey. This paper proposes a possible approach for cooperative hunting based on a biologically-inspired predator/prey model. First, we focus on the control of a single predator/single prey model using Sliding Mode Control (SMC), which guarantees robustness with respect to the system uncertainties and varying environment. Second, we focus on aggregation or flocking formation of multiple predators to hunt prey effectively.

For the single predator/single prey case, the predator should be able to quickly respond and move faster than the prey in order to catch the prey. In the multiple predator case, though, it could be possible to capture the prey even if the prey could move more quickly than the predators because multiple predators can restrict the behavior of the prey by encirclement. In order to successfully encircle the prey, multiple predators should be synchronized before they start to encircle (termed stoop in the biological literature). Otherwise, there is a chance for the prey to escape as

Y.H. Chang is with the Department of Mechanical Engineering, University of California, Berkeley, CA 94720 USA yhchang@berkeley.edu

Prof. Claire Tomlin is with the Department of Electrical Engineering and Computer Sciences, University of California, Berkeley, CA 94720 USA tomlin@eecs.berkeley.edu

Prof. Karl Hedrick is with the Department of Mechanical Engineering and Computer Sciences, University of California, Berkeley, CA 94720 USA khedrick@me.berkeley.edu

in the single predator/single prey case. Synchronization in chaotic dynamic systems has received a great deal of interest in various research fields, and several solutions that treat the problem of chaos synchronization in the framework of nonlinear control theory have been proposed [8][9]. In this paper, we propose SMC to synchronize the motion of UAVs to make dispersed UAVs gather to form a flock. We assume that if the evader is within a radius of some pursuit team members, the task is done.

The rest of this paper is organized as follows: Section II presents a simple planar unicycle model and a design of the controller for a single UAV. A schematic diagram of the overall controller for prey hunting based on the predator-prey behavior in nature is discussed in Section III. Design of the proposed synchronization controller for multiple UAVs is given in Section IV. Numerical examples show that a biologically-inspired strategy of multiple UAVs with synchronization might be a possible approach of effectively hunting an evader. Finally, conclusions are given in Section V.

II. A SIMPLE UNICYCLE MODEL AND CONTROLLER

A. Kinematic Model

In this paper, the UAV is modeled as a unicycle moving in the plane, although the methods presented can be extended the 3-dimensional case. Then, the kinematic model of a UAV is usually described by a simple nonlinear model [10][11]:

$$\begin{aligned} \dot{x}_1 &= u_1 \cos \psi \\ \dot{x}_2 &= u_1 \sin \psi \\ \dot{\psi} &= u_2 \end{aligned} \quad (1)$$

where (x_1, x_2) are the Cartesian locations of the UAV and (u_1, u_2) is the control input encompassing the linear and angular velocities, as shown in Figure 1. Also, $y_1 = x_1$ and $y_2 = x_2$ are defined as outputs. Let $q = [x_1, x_2, \psi]^T \in \mathcal{R}^3$, $g_1(x_1, x_2, \psi) = \begin{bmatrix} \cos \psi \\ \sin \psi \\ 0 \end{bmatrix}$, and $g_2(x_1, x_2, \psi) = \begin{bmatrix} 0 \\ 0 \\ 1 \end{bmatrix}$. Then, we can describe the two input two output system as shown below:

$$\dot{q} = g_1(q)u_1 + g_2(q)u_2 \quad (2)$$

This system is controllable because it is a drift free system and the accessibility distribution (Lie Bracket) has rank 3 as

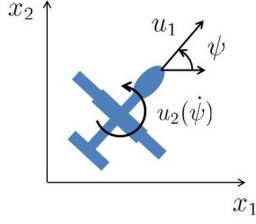


Fig. 1. A simple unicycle model.

shown below [12]:

$$[g_1, g_2] = \frac{\partial g_2}{\partial q} g_1 - \frac{\partial g_1}{\partial q} g_2 = \begin{bmatrix} \sin \psi \\ -\cos \psi \\ 0 \end{bmatrix} \quad (3)$$

$$\text{rank} \begin{pmatrix} \cos \psi & 0 & \sin \psi \\ \sin \psi & 0 & -\cos \psi \\ 0 & 1 & 0 \end{pmatrix} = 3 \quad (4)$$

B. Feedback Linearization Control (FLC) using dynamic extension

The invertibility matrix $J_1(q)$ is clearly singular:

$$\begin{bmatrix} \dot{y}_1 \\ \dot{y}_2 \end{bmatrix} = J_1(q) \begin{bmatrix} u_1 \\ u_2 \end{bmatrix}, \text{ where } J_1(q) = \begin{bmatrix} \cos \psi & 0 \\ \sin \psi & 0 \end{bmatrix} \quad (5)$$

Thus we apply dynamic extension [11][12]: define $u_1 \triangleq x_3$ then, $\dot{x}_3 = u_3$ where u_3 is the acceleration of the UAV. We design a feedback linearization control (FLC) as follows:

$$\begin{bmatrix} \dot{y}_1 \\ \dot{y}_2 \end{bmatrix} = \begin{bmatrix} \cos \psi & -x_3 \sin \psi \\ \sin \psi & x_3 \cos \psi \end{bmatrix} \begin{bmatrix} u_3 \\ u_2 \end{bmatrix} = J_2(q) \begin{bmatrix} u_3 \\ u_2 \end{bmatrix} \triangleq \begin{bmatrix} v_1 \\ v_2 \end{bmatrix}_{FLC} \quad (6)$$

where (v_1, v_2) is a synthetic input pair. Also, the invertibility matrix $J_2(q)$ is nonsingular as long as $x_3 \neq 0$. This is a reasonable assumption as the velocity of the UAV, x_3 , is assumed to be bounded away from zero. Dynamic extension leads to a dynamic controller:

$$\begin{bmatrix} u_3 \\ u_2 \end{bmatrix} = J(q)^{-1} \begin{bmatrix} v_1 \\ v_2 \end{bmatrix}_{FLC} = J(q)^{-1} \begin{bmatrix} -c_1 \dot{y}_1 - c_2 (y_1 - y_{1d}) \\ -c_3 \dot{y}_2 - c_4 (y_2 - y_{2d}) \end{bmatrix} \quad (7)$$

where (y_1, y_2) is a trajectory of pursuer UAV, (y_{1d}, y_{2d}) is a desired trajectory, which represents the trajectory of the evader, and $c_i > 0$. In this paper, we assume that after the pursuer detects the evader, the pursuer can measure the position of the evader, (y_{1d}, y_{2d}) , using for example, a sensor such as a laser scanner.

C. Sliding Mode Control (SMC)

Our simple model is a kinematic model, and thus certain dynamics of pursuit-evasion behavior are not captured. For example, if the evader changes its direction and velocity suddenly, the pursuers cannot dynamically follow these changes because instantaneous changes in linear or angular velocities are not dynamically possible. Also, there might be delay of information, sensor delay or actuator delay. We can consider these terms as model uncertainties or disturbances which affect the kinematics of the pursuer's motion. In order

to make our problem simple, here we assume there is a disturbance in the acceleration dynamics (we will cover a more general case in Sections II-E and II-F):

$$\begin{bmatrix} \ddot{y}_1 \\ \ddot{y}_2 \end{bmatrix} = \begin{bmatrix} \cos \psi & -x_3 \sin \psi \\ \sin \psi & x_3 \cos \psi \end{bmatrix} \begin{bmatrix} u_3 \\ u_2 \end{bmatrix} + \begin{bmatrix} \Delta_1 \\ \Delta_2 \end{bmatrix} \quad (8)$$

where Δ_1, Δ_2 are disturbances, assumed bounded ($|\Delta_i| \leq \alpha_i$). These uncertainties and disturbances motivate our use of sliding mode control (SMC), which can be applied to suppress the effects of modeling uncertainty or disturbance with a high enough gain switching controller. We define a sliding surface as follows:

$$S_1 \triangleq \dot{\epsilon}_1 + \lambda_1 \epsilon_1 = (\dot{y}_1 - \dot{y}_{1d}) + \lambda_1 (y_1 - y_{1d}) \quad (9)$$

$$\begin{aligned} \dot{S}_1 &\triangleq \ddot{\epsilon}_1 + \lambda_1 \dot{\epsilon}_1 = (\ddot{y}_1 - \ddot{y}_{1d}) + \lambda_1 \dot{\epsilon}_1 \\ &= (u_3 \cos \psi - x_3 \sin \psi u_2 + \Delta_1) - \ddot{y}_{1d} + \lambda_1 \dot{\epsilon}_1 \end{aligned} \quad (10)$$

Similarly, we can define $S_2 \triangleq \dot{\epsilon}_2 + \lambda_2 \epsilon_2$ and we can formulate both in matrix form:

$$\begin{bmatrix} \dot{S}_1 \\ \dot{S}_2 \end{bmatrix} = \begin{bmatrix} \cos \psi & -x_3 \sin \psi \\ \sin \psi & x_3 \cos \psi \end{bmatrix} \begin{bmatrix} u_3 \\ u_2 \end{bmatrix} + \begin{bmatrix} -\ddot{y}_{1d} + \Delta_1 + \lambda_1 \dot{\epsilon}_1 \\ -\ddot{y}_{2d} + \Delta_2 + \lambda_2 \dot{\epsilon}_2 \end{bmatrix} \quad (11)$$

We define a Lyapunov function for a MIMO system $V = \frac{1}{2}(S_1^2 + S_2^2)$. If we choose the input $\begin{bmatrix} u_3 \\ u_2 \end{bmatrix} = J_2(q)^{-1} \begin{bmatrix} v_1 \\ v_2 \end{bmatrix}$, and differentiate the Lyapunov function, then

$$\dot{V} = [S_1 \quad S_2] \begin{bmatrix} v_1 - \ddot{y}_{1d} + \Delta_1 + \lambda_1 (\dot{y}_1 - \dot{y}_{1d}) \\ v_2 - \ddot{y}_{2d} + \Delta_2 + \lambda_2 (\dot{y}_2 - \dot{y}_{2d}) \end{bmatrix} \quad (12)$$

where v_1, v_2 are synthetic inputs and we can select as shown below:

$$\begin{bmatrix} v_1 \\ v_2 \end{bmatrix} = \begin{bmatrix} \dot{y}_{1d} - \lambda_1 (\dot{y}_1 - \dot{y}_{1d}) + \ddot{u}_1 \\ \dot{y}_{2d} - \lambda_2 (\dot{y}_2 - \dot{y}_{2d}) + \ddot{u}_2 \end{bmatrix} \quad (13)$$

where $\ddot{u}_1 = -k_1 \text{sgn}(S_1)$ and $\ddot{u}_2 = -k_2 \text{sgn}(S_2)$. Then, equation (12) can be reduced:

$$\begin{aligned} \dot{V} &= [S_1 \quad S_2] \begin{bmatrix} \Delta_1 + \ddot{u}_1 \\ \Delta_2 + \ddot{u}_2 \end{bmatrix} \\ &= S_1 (\Delta_1 - k_1 \text{sgn}(S_1)) + S_2 (\Delta_2 - k_2 \text{sgn}(S_2)) \end{aligned} \quad (14)$$

Considering the worst case uncertainty ($\Delta_1 = \alpha_1 \text{sgn}(S_1)$, $\Delta_2 = \alpha_2 \text{sgn}(S_2)$) and choosing $k_1 (= \alpha_1 + \eta_1)$ and $k_2 (= \alpha_2 + \eta_2)$ then,

$$\dot{V} = S_1 \dot{S}_1 + S_2 \dot{S}_2 \leq -\eta_1 |S_1| - \eta_2 |S_2| \leq 0 \quad (15)$$

where η_i are positive so $\dot{V} \leq 0$ (equality holds only if $S_1 = S_2 = 0$) which means S_1 and S_2 go to zero by the Lyapunov theory (i.e. error dynamics converge to zero). Therefore, we can suppress modeling uncertainty and disturbance. Our sliding mode control becomes:

$$\begin{bmatrix} u_3 \\ u_2 \end{bmatrix}_{SMC} = J_2^{-1} \begin{bmatrix} \dot{y}_{1d} - \lambda_1 (\dot{y}_1 - \dot{y}_{1d}) - (\alpha_1 + \eta_1) \text{sgn}(S_1) \\ \dot{y}_{2d} - \lambda_2 (\dot{y}_2 - \dot{y}_{2d}) - (\alpha_2 + \eta_2) \text{sgn}(S_2) \end{bmatrix} \quad (16)$$

Also, in order to avoid chattering, we can use a smoothing or a saturation function [11]. However, in general, it is hard to measure or estimate $\ddot{y}_{1d}, \ddot{y}_{2d}, \dot{y}_{1d}, \dot{y}_{2d}$ because they are trajectories of the evader.

D. Modified Sliding Mode Control

As we mentioned above, we cannot implement equation (16) in practice because it is hard to measure the velocity and acceleration of the evader ($\dot{y}_{1d}, \dot{y}_{1d}, \dot{y}_{2d}, \dot{y}_{2d}$) and even if we could, they would be subject to uncertainty. Thus, we propose a more practical sliding mode controller:

$$\begin{bmatrix} u_3 \\ u_2 \end{bmatrix}_{new} = J_2(q)^{-1} \begin{bmatrix} v_1 \\ v_2 \end{bmatrix}_{FLC} + J_2(q)^{-1} \begin{bmatrix} \tilde{u}_1 \\ \tilde{u}_2 \end{bmatrix} \quad (17)$$

If we substitute this input in equation (8), then

$$\begin{aligned} \ddot{y}_1 + c_1\dot{y}_1 + c_2y_1 &= c_2y_{1d} + \Delta_1 + \tilde{u}_1 \\ \ddot{y}_2 + c_3\dot{y}_2 + c_4y_2 &= c_4y_{2d} + \Delta_2 + \tilde{u}_2 \end{aligned} \quad (18)$$

Define a new sliding surface $S_1 \triangleq y_1 - y_{1d}$, $S_2 \triangleq y_2 - y_{2d}$ and using the same Lyapunov function, $\dot{V} = S_1\dot{S}_1 + S_2\dot{S}_2$. The dynamics of S_1 is given by:

$$\begin{aligned} \dot{S}_1 &= \dot{y}_1 - \dot{y}_{1d} = \frac{1}{c_1}(-\ddot{y}_1 - c_2y_1 + c_2y_{1d} + \Delta_1 + \tilde{u}_1) - \dot{y}_{1d} \\ S_1\dot{S}_1 &= -\frac{c_2}{c_1}S_1^2 + \frac{1}{c_1}S_1(-\ddot{y}_1 + \Delta_1 + \tilde{u}_1 - c_1\dot{y}_{1d}) \end{aligned} \quad (19)$$

Again, considering the worst case:

$$\begin{aligned} \Delta_1 &= \alpha_1 \text{sgn}(S_1) \\ \ddot{y}_1 &= -\max(|\ddot{y}_1|) \text{sgn}(S_1) \\ \dot{y}_{1d} &= -\max(|\dot{y}_{1d}|) \text{sgn}(S_1) \end{aligned} \quad (20)$$

Selecting $\tilde{u}_1 = -k_1 \text{sgn}(S_1)$, where $k_1 (= \alpha_1 + \max(|\ddot{y}_1|) + c_1 \max(|\dot{y}_{1d}|) + \eta_1)$ is large enough to suppress these terms, (reasonable because the acceleration of motion (\ddot{y}_1) and velocity of evader (\dot{y}_{1d}) are physical quantities so they should be bounded), we can guarantee robustness:

$$S_1\dot{S}_1 \leq -\frac{\eta_1}{c_1}|S_1| \quad (21)$$

Similarly, we can select $\tilde{u}_2 = -k_2 \text{sgn}(S_2)$ to suppress the uncertainty terms ($S_2\dot{S}_2 \leq -\frac{\eta_2}{c_3}|S_2|$). Then, our modified sliding control input is as shown below:

$$\begin{bmatrix} u_3 \\ u_2 \end{bmatrix}_{new} = J_2^{-1} \left(\begin{bmatrix} v_1 \\ v_2 \end{bmatrix}_{FLC} + \begin{bmatrix} -k_1 \text{sgn}(y_1 - y_{1d}) \\ -k_2 \text{sgn}(y_2 - y_{2d}) \end{bmatrix} \right) \quad (22)$$

Therefore, FLC makes $y_1 \rightarrow y_{1d}, y_2 \rightarrow y_{2d}$ and the second term in equation (22) suppresses disturbances effectively. Again, in order to reduce chattering, we can apply a smoothing or a saturation function.

E. Multiple Sliding Surfaces (MSS)

In sections II-C and II-D, we consider uncertainty only in the acceleration because we assume it is dominant. Here, we consider a more general case (consider uncertainty in the dynamics of velocity and acceleration) as shown below:

$$\begin{aligned} \dot{y}_1 &= \dot{x}_1 = u_1 \cos \psi + \Delta_1 \\ \dot{y}_2 &= \dot{x}_2 = u_1 \sin \psi + \Delta_2 \end{aligned} \quad (23)$$

where Δ_1, Δ_2 are disturbances, assumed to be bounded ($|\Delta_i| \leq \alpha_i$). This is a mismatched system but we can handle this

using Multiple Sliding Surface (MSS) [13]. We reformulate our system as shown below:

$$\begin{aligned} \dot{y}_1 &= x_3 \cos \psi + \Delta_1 \triangleq y_4 + \Delta_1 \\ \dot{y}_2 &= x_3 \sin \psi + \Delta_2 \triangleq y_5 + \Delta_2 \\ \dot{x}_3 &= u_3, \quad \dot{\psi} = u_2 \end{aligned} \quad (24)$$

where $y_4 = x_3 \cos \psi$, $y_5 = x_3 \sin \psi$. Differentiating, $\dot{y}_4 = u_3 \cos \psi - x_3 \sin \psi u_2$ and $\dot{y}_5 = u_3 \sin \psi + x_3 \cos \psi u_2$. We define sliding surface $S_1 \triangleq y_1 - y_{1d}$, $S_2 \triangleq y_2 - y_{2d}$ and design a controller as shown below:

$$\begin{aligned} y_{4d} &= -\lambda_1 S_1 - \alpha_1 \text{sgn}(S_1) + \dot{y}_{1d} \\ y_{5d} &= -\lambda_2 S_2 - \alpha_2 \text{sgn}(S_2) + \dot{y}_{2d} \end{aligned} \quad (25)$$

$$S_3 \triangleq y_4 - y_{4d}, \quad S_4 \triangleq y_5 - y_{5d} \quad (26)$$

$$\begin{bmatrix} u_3 \\ u_2 \end{bmatrix} = J_2(q)^{-1} \begin{bmatrix} \dot{y}_{4d} - k_3 S_3 \\ \dot{y}_{5d} - k_4 S_4 \end{bmatrix} \quad (27)$$

Claim: The control input defined by equation (27) guarantees stability and robustness.

Proof: From equation (26), we can differentiate S_3 and S_4 :

$$\begin{bmatrix} \dot{S}_3 \\ \dot{S}_4 \end{bmatrix} = \begin{bmatrix} \cos \psi & -x_3 \sin \psi \\ \sin \psi & -x_3 \cos \psi \end{bmatrix} \begin{bmatrix} u_3 \\ u_2 \end{bmatrix} - \begin{bmatrix} \dot{y}_{4d} \\ \dot{y}_{5d} \end{bmatrix} \quad (28)$$

Substitute equation (27) in equation (28):

$$\begin{bmatrix} \dot{S}_3 \\ \dot{S}_4 \end{bmatrix} = \begin{bmatrix} -k_3 S_3 \\ -k_4 S_4 \end{bmatrix} \quad (29)$$

The dynamics of S_1 is given by:

$$\begin{aligned} \dot{S}_1 &= \dot{y}_1 - \dot{y}_{1d} = y_4 + \Delta_1 - \dot{y}_{1d} = S_3 + y_{4d} + \Delta_1 - \dot{y}_{1d} \\ &= S_3 - \lambda_1 S_1 - \alpha_1 \text{sgn}(S_1) + \Delta_1 \end{aligned} \quad (30)$$

Similarly, the dynamics of S_2 is given by:

$$\dot{S}_2 = S_4 - \lambda_2 S_2 - \alpha_2 \text{sgn}(S_2) + \Delta_2 \quad (31)$$

Plug in equations (29)-(31) to \dot{V} ,

$$\begin{aligned} \dot{V} &= S_1\dot{S}_1 + S_2\dot{S}_2 + S_3\dot{S}_3 + S_4\dot{S}_4 \\ &\leq S_1(S_3 - \lambda_1 S_1) + S_2(S_4 - \lambda_2 S_2) - k_3 S_3^2 - k_4 S_4^2 \\ &= -\lambda_1 S_1^2 - \lambda_2 S_2^2 - k_3 S_3^2 - k_4 S_4^2 + S_1 S_3 + S_2 S_4 \end{aligned} \quad (32)$$

For inequality in equation (32), we consider the worst case $\Delta_1 = \alpha_1 \text{sgn}(S_1)$ and $\Delta_2 = \alpha_2 \text{sgn}(S_2)$. Also, if we choose $k_3 = \lambda_1 + \lambda_3$ and $k_4 = \lambda_2 + \lambda_4$, then

$$\begin{aligned} \dot{V} &\leq -\lambda_1(S_1^2 + S_3^2) + S_1 S_3 - \lambda_2(S_2^2 + S_4^2) + S_2 S_4 \\ &\quad - \lambda_3 S_3^2 - \lambda_4 S_4^2 \end{aligned} \quad (33)$$

which can be made negative definite for a choice of $\lambda_1 > 1/2, \lambda_2 > 1/2$. ■

Therefore, the control using MSS can be used for the general case (the control in Section II-C is limited because we consider uncertainty only for acceleration). However, the difficulties with this scheme are obtaining $\dot{y}_{4d}, \dot{y}_{5d}$ since \dot{S}_1 and \dot{S}_2 involve uncertainty terms (Δ_1, Δ_2). We can handle this problem by numerical differentiation or the use of a low pass filter to smooth the signal.

F. Dynamic Surface Control (DSC)

Swaroop *et al.* [13] proposed a Dynamic Surface Controller (DSC) design method in order to reduce the complexity when MSS is applied. We can apply this method to our problem:

$$\begin{aligned}
 S_1 &= y_1 - y_{1d}, \quad S_2 = y_2 - y_{2d} \\
 \tau_1 \dot{z}_1 + z_1 &= y_{4d}, \quad \tau_2 \dot{z}_2 + z_2 = y_{5d} \\
 S_3 &= y_4 - z_1, \quad S_4 = y_5 - z_2 \\
 \zeta_1 &= z_1 - y_{4d}, \quad \zeta_2 = z_2 - y_{5d} \\
 \begin{bmatrix} u_3 \\ u_2 \end{bmatrix} &= J_2(q)^{-1} \begin{bmatrix} \frac{y_{4d} - z_1}{\tau_1} - \lambda_3 S_3 \\ \frac{y_{5d} - z_2}{\tau_2} - \lambda_4 S_4 \end{bmatrix}
 \end{aligned} \quad (34)$$

A Lyapunov function is given by:

$$V = \frac{1}{2}(S_1^2 + S_2^2 + S_3^2 + S_4^2 + \zeta_1^2 + \zeta_2^2) \quad (35)$$

By Theorem [13], there exists a set of gains and filter times such that system is semi-globally stable (namely, $S_1 \rightarrow 0$, $S_2 \rightarrow 0$, $S_3 \rightarrow 0$, $S_4 \rightarrow 0$, and $z_2 \rightarrow y_{5d}$ which lie inside a ball of controllable radius).

G. Numerical Examples

We focus on a simple example (section (II-B) and (II-C)).

1) *Example1:* Figure 2 shows the simulation results of each controller. We can see that the FLC controller performs well if there is no disturbance or model uncertainty ((a) and (b)). However, the SMC controller is robust even though there is a disturbance. Figure 3 shows the synthetic input for each case ((a), (c) and (d)). Also, it shows that smooth SMC guarantees stability up to a boundary layer (ϕ_r , see error graph (b) and (c) in Figure 3).

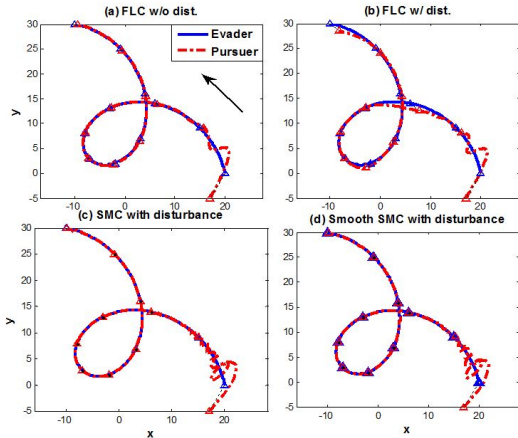


Fig. 2. Trajectory of prey and predator (a) FLC w/o disturbance (b) FLC w/ disturbance (c) SMC w/disturbance (d) Smooth SMC w/disturbance.

2) *Example2:* We can consider the case in which there is a restriction of the input, such as actuator saturation or a maneuver limitation of the aircraft. Figure 4 shows the simulation result of a fast evader/slow pursuer if there is saturation or a limitation of the synthetic input (restriction of maneuver such as maximal rate of turning angle, maximal

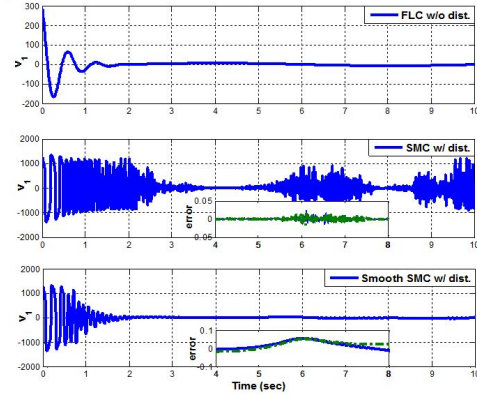


Fig. 3. Synthetic input (a) FLC w/o disturbance (b) SMC w/disturbance (c) Smooth SMC w/disturbance.

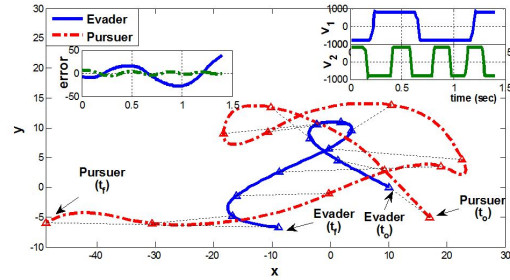


Fig. 4. Swift Evader / Pursuer with maneuver limitation.

speed and so on) of the predator. For example, if the evader has higher mobility, the evader can escape from a single pursuer. In Figure 4, the evader is swift and it can escape the pursuer at the final time t_f because the pursuer loses sight and pursuer cannot know about the evader's trajectory anymore. Therefore, the single pursuer has a limitation in order to follow the fast evader even when the SMC can suppress model uncertainty. This motivates us to consider multiple UAVs and their cooperation for prey hunting.

III. AGGREGATION AND FLOCKING

In Section II, we showed that actuator saturation, and the restriction of maneuvers, degrades control performance of SMC. Therefore, a single pursuer's success is limited, especially for a more capable evader. However, collaboration can help. In biology, flocking can be defined as a collective motion of a large number of self-propelled agents with a common group objective [14]. This flocking behavior is a basic behavior among many swarms or animals in nature. For example, most social predators are facultative social predators, meaning that they are capable of catching some prey while hunting alone and also of hunting socially to take down larger prey (Figure 5 [15]). This collective behavior can be applied to multi-agent systems. Here, we adapt biological behaviors to multiple UAVs. For example, once the pursuer UAV (master) detects the evader (Prey) (Figure 6(a), M1), then it sends a message to other pursuers (slave, S1 and S2) in order to coordinate a group of agents that are initially



Fig. 5. Facultative social predators: lions hunting a wildebeest.

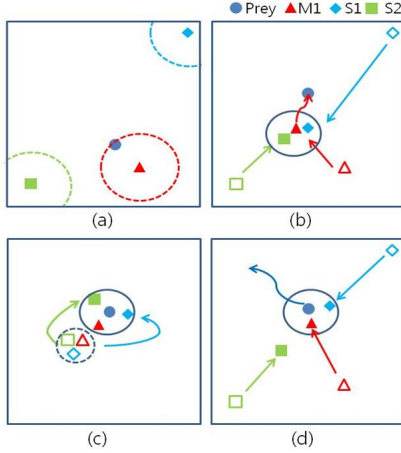


Fig. 6. (a) Surveillance (b) Stalk / Synchronize (c) Capture (d) step (b) and (c) simultaneously.

at random positions and directions. This is a reasonable approach because only the master UAV is assumed to know the position of the prey, and each UAV knows the other UAV location. During the coordination, the master UAV stalks the prey (Figure 6(b), stalk and flock). Then, once the UAVs converge or construct a structured formation, the pursuers can split and encircle the evader (Figure 6(c), flock splitting and stoop). Figure 7 shows an overall architecture of the controller. In this paper, we consider step (b). To address the question of why the slave UAVs are synchronized with the master UAV and not the evader, one can point to three main reasons. First, slave UAVs do not know the location of the evader. Of course, the master UAV in general can send them its location but there could be a delay or a disturbance since the master UAV is following the evader. On the other hand, all UAVs communicate with each other so they know the location of others. Therefore, it is easy to construct the formation. Second, if the slave UAVs synchronize with the evader (basically, a combination of step (b) and (c) simultaneously in Figure 6 (d)), there are many chances for evader escape because the pursuers are not synchronized. For example, if M1 and S1 converge quickly to the evader before S2 converges (Figure 6 (d)), then the evader can escape by turning to the other side of M1 and S1. However, if we do step (b) and (c) sequentially, namely synchronize and later incorporate stoop, it is a more effective way to hunt prey. Third, the gain of SMC (k) increases with increasing uncertainty. Without loss of generality, the uncertainty between predator and prey is higher than the

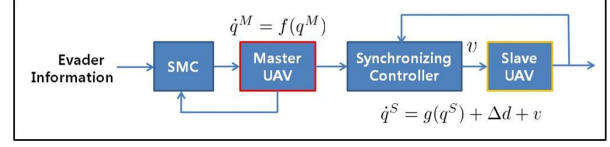


Fig. 7. Block diagram of the overall controller.

uncertainty between Master and Slave UAVs because we know model dynamics of our UAVs. Also, if the gain is high, it is easy to saturate if there is actuator limitation.

IV. A BIOLOGICALLY-INSPIRED MOTION SYNCHRONIZATION

We can formulate motion synchronization using SMC [9]:

$$\begin{aligned}
 [\text{Master}] \quad & \dot{q}^M = f(q^M) \\
 [\text{Slave}] \quad & \dot{q}^S = g(q^S) + \Delta d + v \\
 [\text{Goal}] \quad & \lim_{t \rightarrow t_f} |q^S - q^M| = 0 \quad (\text{Synchronize}) \quad (36)
 \end{aligned}$$

where M represents master UAV, S represents slave UAVs and $\Delta d (\leq \beta)$ is a disturbance or model difference from each UAV. Also, if our UAVs are homogeneous, which means that all UAVs are the same type of UAV, $g(\cdot)$ can be replaced by $f(\cdot)$. We can define a sliding surface as shown below:

$$s \triangleq e = q^S - q^M \quad (37)$$

$$\dot{s} = \dot{q}^S - \dot{q}^M = g(q^S) + \Delta d + v - f(q^M) \quad (38)$$

where v is an input to the slave UAVs to synchronize with the master UAV. We can choose v which guarantees a sliding mode surface ($s\dot{s} < 0$) as shown below:

$$v = -(g(q^S) - f(q^M)) - k \text{sgn}(s) \quad (39)$$

$$\dot{s} = \Delta d - k \text{sgn}(s) \leq -\eta \text{sgn}(s) \quad (40)$$

$$s\dot{s} \leq -\eta |s| \quad (41)$$

where $k (= \beta + \eta)$ is chosen to satisfy the reaching condition which guarantees the states are on the sliding surface for the worst case ($\Delta d = \beta \text{sgn}(s)$).

A. Example 1

We assume the GPS sensor gives UAV position information in order to verify the synchronization scheme. Figure 8 show multiple(3) UAVs and 1 prey(evader) case. Master, close to the prey, can detect the evader and start to follow (stalk). Then, the synchronizing controller makes the other slave UAVs (Slave1, Slave2) follow Master. Figure 8 shows the position and direction of each UAV. Note that first, Slave1 and Slave2 converge to Master, and then, Master converges to the prey with a different converging time because they have different SMC gains.

B. Example 2

Figure 9 shows simulation results of the fast evader case (discussed in Figure 4). The only difference is that we have 2 more UAVs. Also, we consider actuator saturation of the master UAV. Figure 9 shows that all UAVs encircle the prey and restrict prey behavior. Therefore, motion synchronization can hunt prey more effectively in a short time.

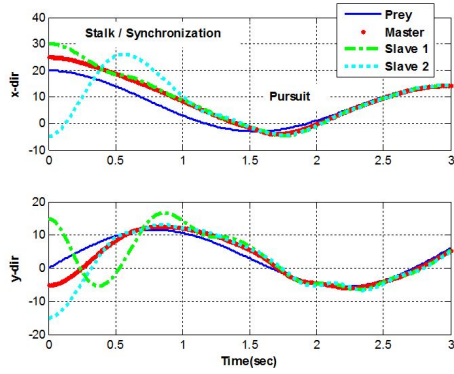


Fig. 8. Position of each UAV during the motion synchronization and pursuing the prey (Example 1).

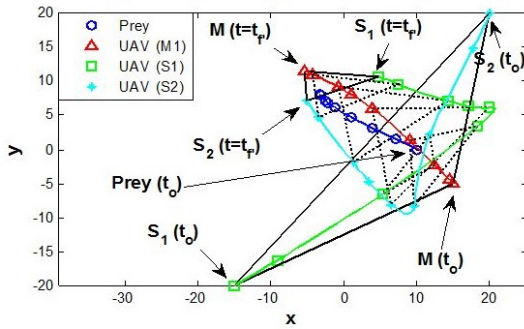


Fig. 9. Motion synchronization can hunt prey more effectively by encircling the prey and restricting the prey behavior (Example 2).

C. Example 3

Figure 10 shows simulation results if there are limitations on the motion of all UAVs (master and slaves). It shows that even if motion synchronization has not yet converged, pursuers can hunt prey by encirclement. Hence, this specific example shows that there is a more chance to hunt prey by restricting the prey behavior.

V. CONCLUSIONS

A simple unicycle model was analyzed using a nonlinear control scheme. We proposed a Feedback Linearization Controller (FLC) and a Sliding Mode Controller (SMC) for a single UAV. Also we proposed a practical SMC and showed the performance of each controller by simulation results. Moreover, we cover the general case using a Multiple Sliding Surface (MSS) controller and Dynamic Surface Controller (DSC). We show the limitation of a single UAV to pursue an evader and proposed a biologically-inspired motion synchronization controller using SMC for multiple UAVs. Simulation results show that multiple UAVs can hunt prey more effectively even though there are maneuver limitations.

VI. ACKNOWLEDGMENTS

The first author would like to thank support from STX foundation from Korea. Also, the authors have benefitted greatly from discussions of this problem with Selina Pan

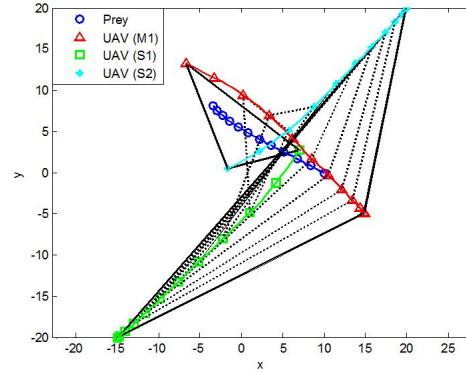


Fig. 10. Motion synchronization if there are limitations on the motion of all UAVs (Example 3).

and Shih-Yuan Liu. This research was supported by ONR under the HUNT MURI program.

REFERENCES

- [1] J. M Eklund, J. Sprinkle, and S. Sastry, "Implementing and Testing a Nonlinear Model Predictive Tracking Controller for Aerial Pursuit Evasion Games on a Fixed Wing Aircraft", Proceedings of American Control Conference (ACC) 2005, Portland, OR, June, 8-10, 2005.
- [2] D. Shim, H. Chung, H. J. Kim, and S. Sastry, "Autonomous Exploration in Unknown Urban Environments for Unmanned Aerial Vehicles", AIAA GN&C Conference, San Francisco, August 2005.
- [3] W.-K. Chen, Linear Networks and Systems (Book style). Belmont, CA: Wadsworth, 1993, pp. 123135.
- [4] J. Tisdale, Zu Kim and K. Hedrick, "An Autonomous System for Cooperative Search and Localization using Unmanned Vehicles", Proceedings of the AIAA Guidance, Navigation and Control Conference, Honolulu, Hawaii, August 2008.
- [5] M. Ji, A. Muhammad, and M. Egerstedt, "Leader-Based Multi-Agent Coordination: Controllability and Optimal Control", American Control Conference (ACC) 2006, Minneapolis, MN, June, pp 1358-1363, 2006
- [6] R. Olfati-Saber. "Flocking for multi-agent dynamic systems: Algorithms and theory", IEEE Trans. Automat. Contr., 51(3):401420, March 2006
- [7] A. Jadbabaie, J. Lin, and A. S. Morse. "Coordination of groups of mobile autonomous agents using nearest neighbor rules", IEEE Trans. Automat. Contr., 48(6):9881001, June 2003
- [8] V. Gazi and K.M. Passino, "A Class of Attraction/Repulsion Functions for Stable Swarm Aggregations", Int. Journal of Control, Vol. 77, No.18, Dec. 2004, pp 1567-1579
- [9] H.N. Agiza and M.T. Yassen, "Synchronization of Rossler and Chen chaotic dynamical systems using active control", Physics Letter A, Vol. 278, Issue 4, pp 191-197
- [10] M. Roopaei and M. Z. Jahromi, "Synchronization of two different chaotic systems using novel adaptive fuzzy sliding mode control", Chaos 18, 033133 (2008); doi:10.1063/1.2980046
- [11] J. K. Hedrick, ME237 lecture notes, UC Berkeley, Spring 2010. <http://www.me.berkeley.edu/ME237/>
- [12] J. Slotine, and W. Li, 1991, Applied Nonlinear Control (Prentice-Hall)
- [13] S. Sastry, 1999, Nonlinear Systems: Analysis, Stability, and Control, Springer
- [14] D. Swaroop, J.K. Hedrick, P.P. Yip, and J.C. Gerdes, "Dynamic Surface Control for a Class of Nonlinear Systems", IEEE Trans. Automat. Contr., VOL. 45, NO. 10, Oct 2000
- [15] P. E. Stander, "Cooperative hunting in lions: the role of the individual", Behavioral Ecology and Sociobiology, Volume 29, Number 6, February, 1992 <http://naturepl.com>